Applied Mathematics & Information Sciences
An International Journal

© 2012 NSP
Natural Sciences Publishing Cor.

Semi-supervised Ultrasound Image Segmentation Based on Direction Energy and Texture Intensity

Ting Yun[1,2]

[1] School of Computer Science Technology, SouthEast University, Nanjing, 210096, China
[2] School of Information Science Technology, Nanjing Forestry University, Nanjing, 210037, China

Received: Jul 20, 2011; Revised Oct. 14, 2011; Accepted Oct. 3, 2011
Published online: 1 August 2012

Abstract: For the ultrasound images accurate segmentation problem, this paper proposes a novel SVM semi-supervised segmentation method based on major features in curvelet domain. Firstly, ultrasound images were decomposed into different directions and frequencies in the curvelet domain, then the cauchy model was used to simulate curvelet coefficients distribution, thus the main distribution of the curvelet coefficients were extracted to reduce the algorithm time complexity; Secondly after curvelet inverse transform we designed texture analysis method to distinguish texture intensity of every blocks among each sub-bands, then elected maximum K numbers energy sub-bands accroding to the strong texture characteristic, followly extracted features such as: angular second moment, contrast, correlation, entropy, variance, mean, adverse moments, etc from these maximum energy sub-bands, thereby calculating data amount was reduced and algorithm real-time performance was improved; Finally we designed semi-supervised SVM classifier and took the expert manual tagging map as reference standards, compared with the results of moment method and active contour model, experimental data show that our algorithm for ultrasound images pathological region segmentation has better accuracy and effectiveness.

Keywords: Ultrasound images, Curvelet transform, Texture analysis, Direction energy, Semi-supervised Segmentation.

1. Introduction

Medical ultrasound image is an important type of medical images and is widely used in medical diagnosis, Compared with other medical imaging methods, Ultrasound imaging has the advantages of non-traumatic to human body, real-time display, low cost, ease to use. As an ideal non-invasive diagnosis method, It has broad prospects for development. However, because of the principle of imaging factors lead to insufficient grayscale display range or unreasonable gray distribution, so the ultrasound images auxiliary diagnosis effect is constrained, especially in some local details, if difference of pathological regions gray level are not obvious, that will bring a lot of difficult to detect. In order to improve ultrasound images quality and enhance the readability of ultrasound image local details, make images suitable for human eyes observation or machine analysis, in recent years automatic pathological area segmentation algorithm has become the research focus.

In recent years some scholars dealt with the ultrasound image segmentation in the frequency domain, such as literature [1] used wavelet decomposition to achieve wavelet coefficients, then combined with neural network method to process segmentation problem. literature [2] constructed an accurate ultrasound image segmentation algorithm in the wavelet domain with the Chan-Vese model, literature [3] combined the local histogram and wavelet transform to locate the position of breast lesions. literature [4] proposed a new method which combined texture and shape as the prior information, then energy equation was constructed and texture of pathological area was classified by the shape parameter and Gabor filter coefficients. Other researchers processed ultrasound image in the space domain, literature [5] proposed segmentation algorithm based on gray probability density function and fast matching ideas for vascular image, Literature [6] constructed an image segmentation method based on graph theory, which has the advantages of robust to noise, sensitive to the blurred edge, low residual error rate and fast calculation speed. After remove speckle noise, literatures [7–9] adopted active contour model combining with prior information such as shape texture color to complete pathology region di-

* Corresponding author: e-mail: njyunting@qq.com

© 2012 NSP
Natural Sciences Publishing Cor.

vision. Christodou [10] used ten different texture feature include first-order statistics, gray-level co-occurrence matrix, gray differential statistics, neighborhood gray difference matrix, statistical feature matrix, texture energy spectrum, characteristic of fractal dimension, power spectrum and shape parameters to extract carotid atherosclerotic plaques, then adopted K-neighboring method to complete separation. literatures [13–15] used a variety of moments to analyze image texture features, then gabor energy, fish identification and active contour models are combined with features for image segmentation. The article [16] focused on comparing several multi-resolution texture analysis methods which include wavelet, ridgelet, and curvelet. The comparision are extensively tested and results are compared with standard texture classification algorithms. Experiment results show that using curvelet-based texture features significantly improves the classification effect in CT scans.

In this paper curvelet coefficients of ultrasound images are got by curvelet transform, cauchy distribution is used to extract main distribution curvelet coefficients and texture intensity of different regions in curvelet subbands are analysed, then these coefficients are brought into the SVM classifier and the error rate is adjusted through iterative modification, thereby we choose the most optimal SVM parameters to complete ultrasound image segmentation, finally comparison with existing algorithms, the validity of our scheme is verified.

2. Ultrasound image segmentation

2.1. Curvelet transform

Curvelet transform provide a new multi-scale image representation method, through curvelet transform, images will decompose into subbands with scale and direction informations, so it has high performance in image segmentation and texture classification that wavelet not own. In this paper we used multi-resolution and multi-direction fine characteristics that obtained by curvelet transform for ultrasound image segmentation. Curvelet transform in R^2 can be defined as follow: We define that x is a spatial variable, ω is a frequency-domain variable, r and θ are radius and angle in polar coordinates. $W(r)$ is a radial window and $V(r)$ is an angular window, they are all smooth, nonnegative and with real-values, and supported in the interval $r \in (3/4, 3/2)$ and $t \in (-1/2, 1/2)$:

$$\sum_{j=-\infty}^{\infty} W^2\left(2^j r\right) = 1 \quad , r \in (3/4, 3/2) \tag{1}$$

$$\sum_{j=-\infty}^{\infty} V^2\left(t - l\right) = 1 \quad , t \in (-1/2, 1/2)$$

For each $j \geq j_0$, a frequency window U_j in the Fourier domain is defined by the support of W and V , U_j is

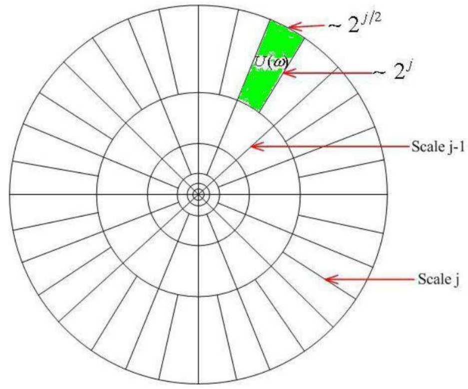

Figure 1 Curvelets in Fourier frequency.

defined in the Fourier domain by:

$$\{U_j(r,\theta) = 2^{-3j/4} W(2^{-j}r) V\left(\frac{2^{[j/2]}\theta}{2\pi}\right) \tag{2}$$

where $[j]$ is the integer part of j . In fact, the support of U_j is a polar "wedge". The symmetrized version of (2), namely $U_j(r,\theta) + U_j(r,\theta+\pi)$, is used in order to obtain real-valued curvelets.

Now the waveform $\varphi_j\left(x\right)$ defined by mean of its Fourier transform $\hat{\varphi}_j\left(x\right) = U_j\left(\omega\right)$. As "mother" wavelet, φ_j is thought to be a "mother" of curvelet, and all curvelets at scales 2^{-j} are obtained by rotations and translations of φ_j. To define the curvelets, symbols θ_l and k are defined as follow: $\theta_l = 2\pi \cdot 2^{-[j/2]} \cdot l$, with $l = 1, 2, ...$ such that $0 \leq \theta < 2\pi$; $k = (k_1, k_2) \in Z^2$. Here, θ_l is equispaced sequence of rotation angles and k the sequence of translation parameters. Then, the curvelet can be defined at scale 2^{-1}, orientation θ_l and position $x_k^{(j,l)} = R_{\theta l}^{-1}\left(k_1 \cdot 2^{-j}, k_2 \cdot 2^{-j/2}\right)$ by

$$\varphi_{j,l,k}\left(x\right) = \varphi_j\left(R_{\theta l}\left(x - x_k^{(j,l)}\right)\right) \tag{3}$$

For a given image $I \in L^2\left(R^2\right)$, the curvelet coefficients is defined by

$$c(i,l,k) = \langle I, \varphi_{j,l,k} \rangle = \int_{R^2} I\left(x\right) \overline{\varphi_{j,l,k}\left(x\right)} dx \tag{4}$$

Digital curvelet transforms can also be operated in the frequency domain, and it will be useful to apply Plancherel's theorem and express the inner product as the integral over the frequency plane:

$$\begin{aligned} c\left(i,l,k\right) &= \tfrac{1}{(2\pi)^2} \int \hat{I}\left(\omega\right) \overline{\hat{\varphi}_{j,l,k}\left(\omega\right)} d\omega \\ &= \tfrac{1}{(2\pi)^2} \int \hat{I}\left(\omega\right) U_j\left(R_{\theta l}\omega\right) e^{i\left\langle x_k^{(j,l)}, \omega\right\rangle} d\omega \end{aligned} \tag{5}$$

In order to realize the curvelet transform, unequally spaced fast fourier transform(USFFT) algorithm is adopt-

© 2012 NSP
Natural Sciences Publishing Cor.

ed in our algorithm, it is a fast discrete curvelet transform method [11,12], The realization process is divided into four steps:

1) For a given two-dimensional image $I\left[t_1,t_2\right], t_1,t_2 \in \Omega_{image}$ in Cartesian coordinates, we used two-dimensional fast Fourier transform (2DFFT), and get two dimensional frequency domain representation: $\hat{I}\left[n_1,n_2\right], -n/2 \leq n_1,n_2 \leq n/2$;

2) In the frequency domain, for each scale and angle.., re-sampling $\hat{I}\left[n_1,n_2\right]$ will get $\hat{I}\left[n_1,n_2-n_1\tan\theta_1\right]$, (n_1,n_2) $\in P_j$, where $P_j=\begin{Bmatrix}(n_1,n_2): n_{1,0}\leq n_1<n_{1,0}+L_{1,j},\\ n_{2,0}\leq n_2<n_{2,0}+L_{2,j}\end{Bmatrix}$ is parameter about 2^j, $L_{2,j}$ is parameter about $2^{j/2}$, They represent length and width about support interval of $\tilde{U}_j\left[n_1,n_2\right]$;

3) The interpolated $\hat{I}$ multiply with window function $\tilde{U}_j$, then $\tilde{I}_{jl}$ will get:

$$\tilde{I}_{jl}\left[n_1,n_2\right]=\hat{I}\left[n_1,n_2-n_1\tan\ theta_1\right]\tilde{U}_j\left[n_1,n_2\right];$$

4) For the $\tilde{I}_{jl}$ do inverse 2DIFFT transformation, so discrete curvelet coefficients $c^D\left(j,l,k\right)$ are got.

The ultrasound image I is taken USFFT transform, according to scale j and direction l ,then I is decomposed into 5 layers, both the 1th layer (the lowest frequency) and 5th layer (the highest frequency) have only 1 direction, and both the 2th layer and 3th layer have 32 directions, the 4th layer has 64 directions. All layers with different directions can represented as $\{1,32,32,64,1\}$, among them at regular intervals choose partial $\{1,16,16,0,1\}$ directions as the ultrasound image features. But the count of these directions data is enormous, in order to reduce the algorithm computational load and time complexity, we adopted three strategies. Firstly we analyzed the curvelet coefficients distribution obey what probability models, then extract main distribution curvelet coffients. Secondly after inverse curvelet transform, these direction data of different layers convert into 34 sub-bands, through calculating texture intensity of every blocks among each sub-band to determine the maximum energy subbands. Finally according to the above method efficiently and refinedly extract main image features to form feature vector which bring to the SVM classifier for image segmentation.

2.2. Curvelet coefficient main distribution

In this section, three kinds of distribution function are used to simulate curvelet coefficients distribution, specific to:

1) Generalized Gaussian distribution (GGD):

$$f\left(x,\bar{\mu},s,u\right)=\frac{s}{2\beta\Gamma\left(1/s\right)}\exp\left\{-\left[\frac{|x-\bar{\mu}|}{u}\right]^{\alpha}\right\} \quad (6)$$

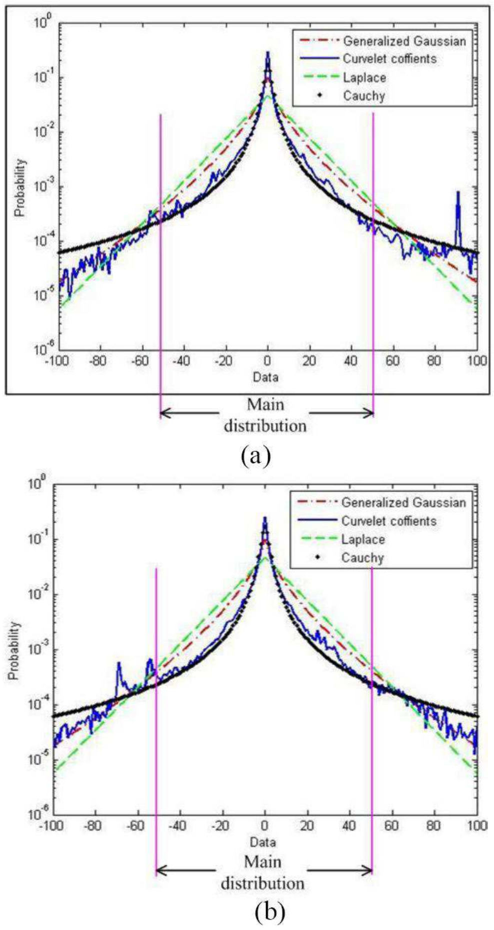

Figure 2 Histogram and estimated primary distribution of curvelet coefficients, (a) ultrasound image1 curvelet coefficients distribution, (b) ultrasound image2 curvelet coefficients distribution.

where x $\in I$,$\Gamma\left(\cdot\right)=\int_0^{\infty}e^{-t}t^{z-1}dt, u=\sqrt{\frac{\sigma^2\Gamma(1/a)}{\Gamma(3/a)}}$ $s,\sigma>0$; $\bar{\mu}$ is GGD mean value, σ^2 is variance, s is shape parameter, u is scale parameter.

2) Laplase distribution:

$$f\left(x\right)=\frac{b'}{2}\exp\left(-b'\cdot|x|\right), x\in I \quad (7)$$

where $b'=\sqrt{2}/\sigma$.

3) Cauchy distribution:

$$f\left(x,x_0,\bar{\gamma}\right)=\frac{1}{\pi}\left[\bar{\gamma}\Big/\left(\left(x-x_0\right)^2+\bar{\gamma}^2\right)\right] \quad (8)$$

Figure 2 (a) and (b) show the estimated and the observed densities of the curvelet coefficients of two random ultrasound images on log scale. From the Figure 2, it can be seen that the histogram is clearly non-Gaussian whereas the Cauchy model is closer to the actual histogram, then

© 2012 NSP
Natural Sciences Publishing Cor.

primary distribution curvelet coefficients (as shown in Figure 2, the part between purple lines) are taken out as the characteristic quantity that will be used in the following section. Through inverse curvelet transform these primary distribution curvelet coefficients following convert into 34 sub-bands, each sub-band with (512×512) size.

2.3. *Determination of texture strength and main direction*

The image texture can divide into two class: strong texture and weak texture. The regions S_1 with strong texture represents the texture characteristics is obvious, just opposite to the weak regions S_2; after curvelet inverse transform direction data convert into $N_{dir} = 34$ sub-bands, and for each sub-band is divided into non-overlapping M numbers blocks X_p,$p = 1, 2, 3...M$; every block X_p contains N_{ele} pixels, N_{ele}, $M = 32{*}32$, $N \times N = 16{*}16$; Each block in its sub-bands can denote by $Curvelet[z_1, z_2]$ $z_1 = 1 \ldots N_{dir}$ $z_2 = 1 \ldots N_{ele}$. then the following parameters are calculated:

1) Each sub-band energy:

$$E_{z_1} = \sum\nolimits_{z_2=1}^{N_{ele}} \left(Curvelet_{X_p}[z_1, z_2]\right)^2 \tag{9}$$

2) Maximum sub-band energy:

$$K_p = \arg\max_{z_1}(E_{z_1}) \tag{10}$$

3) Block average energy of all sub-bands is defined as:

$$ME_{z_1}(p) = \frac{\sum_{z_1=1}^{N_{dir}} \left(\sum_{z_2=1}^{N_{ele}} \left(Curvelet_{X_p}[z_1, z_2]\right)^2 - D_{z_1}^2\right)}{N_{dir}} \tag{11}$$

where $\mathrm{D}_{z_1} = \frac{\sum_{z_2=1}^{N_{ele}} Curvelet[z_1,z_2]}{N_{ele}}$

4) Each block energy variance is defined as:

$$VarE_{z_1}(p) = \sum\nolimits_{z_1=1}^{N_{dir}} (E_{z_1} - DE)/N_{dir} \tag{12}$$

where DE = $\sum_{z_1=1}^{N_{dir}} E_{z_1}/(N_{dir} + 1)$

Applying above parameters, each block X_p is divided into strong texture S_1 and weak textures S_2:

$$\begin{cases} X_p \in S_2 \ \ when \ \ ME_{z_1}(p) > T_1 \ \ and \ \ VarE_{z_1}(p) < T_2 \\ X_p \in S_1 \ \ other \end{cases}$$

where $T_1 = 3 \times \frac{\sum_{p=1}^{M} ME(p)}{M}$,

$$T_2 = \frac{4}{5}\max(VarE_{z_1}(p)) - \frac{1}{5}\min(VarE_{z_1}(p)) \tag{13}$$

Through above steps strong texture blocks of each sub-band can be determinated, then we can choose the maximum energy direction which contains greater number of strong texture blocks. Through voting mode we can select the maximum energy directional. for example, as shown in Figure 3. $z_1 = 1, z_2 = 2$ are two directional sub-bands, the red litter square represents the current block X_p has strong texture, define the maximum energy sub-band which contains largest quantity of red squares, such as subband2 is a major energy directional subband because it contains more red blocks than subband1.

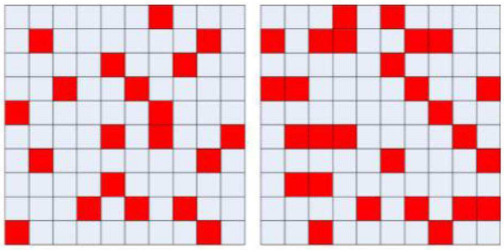

Figure 3 Election of the largest energy subbands.

2.4. *Features extraction*

After main distribution curvelet coffients extraction, every strong texture blocks $\hat{X}_p$ that belong to major energy directional subbands are chose for the following feature calculation:

1) angular second moment:

$$w_1 = \sum_{d_1=1}^{N} \sum_{d_2=1}^{N} \left(\hat{X}_p\right)^2 \quad N_{ele} = N \times N \tag{14}$$

2) contrast:

$$w_2 = \sum_{d_1=1}^{N} \sum_{d_2=1}^{N} n^2 \hat{X}_p\left(d_1, d_2\right), \quad |d_1 - d_2| = n \tag{15}$$

d_1 is the abscissa and d_2 is the ordinate.

3) correlation:

$$w_3 = \left(\sum_{d_1=1}^{N} \sum_{d_2=1}^{N} \left(d_1 d_2\right) \hat{X}_p\left(d_1, d_2\right) - \mu_1 \mu_2 \right) \Big/ \sigma_1^2 \sigma_2^2 \tag{16}$$

where $\mu_1 = \sum\limits_{d_1=1}^{N} d_1 \sum\limits_{d_2=1}^{N} \hat{X}_p\left(d_1, d_2\right)$

$$\mu_2 = \sum_{d_2=1}^{N} d_2 \sum_{d_1=1}^{N} \hat{X}_p\left(d_1, d_2\right)$$

$$\sigma_1^2 = \sum_{d_1=1}^{N} \left(d_1 - \mu_1\right)^2 \sum_{d_2=1}^{N} \hat{X}_p\left(d_1, d_2\right)$$

© 2012 NSP
Natural Sciences Publishing Cor.

$$\sigma_2^2 = \sum_{d_2=1}^{N} (d_2 - \mu_2)^2 \sum_{d_1=1}^{N} \hat{X}_p(d_1, d_2)$$

4) entropy:

$$w_4 = -\sum_{d_1=1}^{N} \sum_{d_2=1}^{N} \hat{X}_p(d_1, d_2) \log \hat{X}_p(d_1, d_2) \qquad (17)$$

$Curvelet_{\hat{X}_p} = \{w_1, w_2, w_3, w_4\}$ is composed by these features, therefore each pixel of ultrasound image is correspond to the eigenvectors $\tilde{x} = Eigenvectors_{\hat{X}_p} = \left\{Curvelet_{\hat{X}_p}\right\}$ then brought into SVM classifier for the medical ultrasonic image segmentation.

2.5. Semi supervised segmentation based on SVM

Training sample set has K samples of two types, can be expressed as:

$$(\tilde{x}_1, y_1), (\tilde{x}_2, y_2), ..., (\tilde{x}_k, y_k), y \in \{+1, -1\} \qquad (18)$$

The principle of SVM algorithm is to find the maximum distance between the two class and define the optimal classification hyper-plane, so the two class is separated, classification hyper-plane can be expressed as:

$$\cdot\phi(\tilde{x}) + b = 0 \qquad (19)$$

Where w is the weight vector of the classification plane, b is offset, ϕ make $\tilde{x}_k$ mapped into the high dimensional feature space, also it used to construct the optimal separating plane in high-dimensional space. In order to ensure that all the samples are correctly classified, penalty term $C' \sum_{i=1}^{k} \xi_i$ is added into the minimum target $\frac{1}{2}\|w\|^2$, forming the objective function is:

$$\frac{1}{2}\|\bar{w}\|^2 + C' \sum_{i=1}^{k} \xi_i \qquad (20)$$

The constraint condition of function (20) is

$$y_i \{[w \cdot \phi(\tilde{x}_i)] + b\} \geq 1 - \xi_i,\ i = 1, 2, ..., k,\ \xi_i \geq 0 \qquad (21)$$

in Formula (20), C' is penalty coefficient; ξ_i is the slack variable. Then acquisition the optimal plane problems is converted into convex quadratic programming optimization problems through lagrange function, That is

$$\begin{cases} \max \sum^{k=i=1} \alpha_i - \frac{1}{2} \sum_{i=1}^{k} \sum_{j=1}^{k} \alpha_i \alpha_j y_i y_j K(\tilde{x}_i, \tilde{x}_j) \\ \sum_{i=1}^{k} y_i \alpha_i = 0,\ \alpha_i \geq 0,\ i = 1, 2, ..., k \end{cases} \qquad (22)$$

in formula(22): α_i is the corresponding Lagrange multiplier; $K(\tilde{x}_i, \tilde{x}_j) = \phi(\tilde{x}_i)\phi(\tilde{x}_j)$ is the kernel function. formula(22) is a quadratic function optimization problem and exist the unique solutions, according to the constraint condition (20) let the optimal solution is $\alpha^0 = (\alpha_1^0, ..., \alpha_k^0)$, so the SVM classification discriminant function is got:

$$f(x) = \mathrm{sgn}\left(\sum_{i=1}^{k} y_i \alpha_i^0 K(\tilde{x}_i, \tilde{x}_j) - b_0\right) \qquad (23)$$

where b_0 is classification threshold. In function (23) commonly used kernel functions include such as: linear kernel function, polynomial function, radial basis function and Sigmoid kernel function. as follows:

$$K(x_i, x_j) = (\tilde{x}_i \cdot \tilde{x}_j)$$

$$K(\tilde{x}_i, \tilde{x}_j) = (\gamma(\tilde{x}_i \cdot \tilde{x}_j) + r')^d, \gamma > 0$$

$$K(\tilde{x}_i, \tilde{x}_j) = \exp\left(-\gamma\|\tilde{x}_i - \tilde{x}_j\|^2\right), \gamma > 0$$

$$K(\tilde{x}_i, \tilde{x}_j) = \tanh[\gamma(\tilde{x}_i \cdot \tilde{x}_j) + r'], \gamma > 0$$

where γ is Gamma coefficients of the kernel function, d is polynomial coefficients; r' is the offset in the radial basis function and sigmoid kernel function.

3. Experiment

In Figure 4, the first line is the training set and the corresponding expert manually labeling segmentation results; in this line (a)1 (a)2 and (a)3 represent training samples; (b)1 (b)2 and (b)3 represent expert manually labeling; The following three lines show our algorithm experiment, (c) represent different testing ultrasound images that to be segmented, (d) represent strong texture blocks of each ultrasound images, the black blocks in Figure 4(d) have the weak texture intensity. (e) represent every ultrasound image final segmentation results, in each result the white line represents the edge of experts manually mark the location of the tumor, the black region is the segmentation results of our method.

Followly true positive (TP) regions which not only belong to actual pathological regions but also belong to algorithm segmentation regions are defined, false positive (FP) regions also defined which belong to the algorithm segmentation regions but not belong to actual pathological regions. false negative (FN) regions are defined which belong to actual pathological region but not belong to the algorithm segmentation regions. According to these three properties, five quantization segmentation parameters are defined:

Accuracy:

$$C_{Acc} = \frac{|TP - FP|}{TP + FN} \qquad (24)$$

© 2012 NSP
Natural Sciences Publishing Cor.

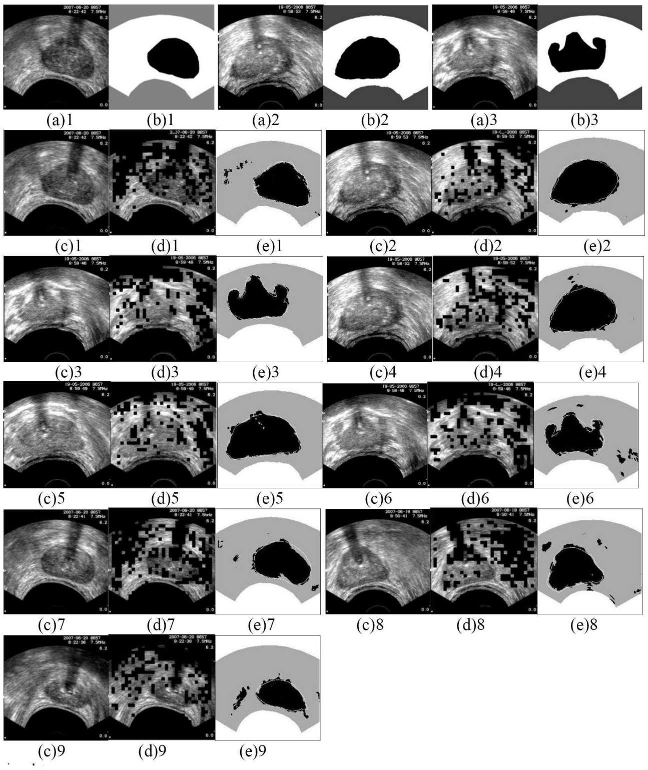

Figure 4 segementation results.

True positive ratio (TPR):

$$C_{TPR} = \frac{TP}{TP + FN} \tag{25}$$

Fractional area difference (FAD):

$$C_{FAD} = \frac{|FP - FN|}{TP + FN} \tag{26}$$

False positive ratio (FPR):

$$C_{FPR} = \frac{FP}{TP + FN} \tag{27}$$

Similarity (SI):

$$C_{SI} = \frac{TP}{TP + FN + FP} \tag{28}$$

C_{TPR} value is larger, our segmentation results cover higher percentage of actual pathological region; C_{FPR} value is smaller, then segmentation area is less error; C_{SI} value is larger, that our segmentation result is closer to the manual label area. Table 1 lists the clinical ultrasound image segmentation results of different methods, GLCM represent Gray-level Co-occurrence Matrix method, it can be seen from the experimental data, our method results about C_{TPR} index are more than 90 percent, which prove our segmentatiobn results can cover most of the actual tumor region, the C_{FPR} index show that our method with low error rate of partitioning tumor region and high accuracy of segmentation. Comparing with the literatures [13–15] method, C_{SI} index shows our method obtained better segmentation effect. On the time complexity, due to the main distribution curvelet coefficients are extracted, so the average computation time is reduced of 25 percent.

Table 1 Comparison of experimental results.

Comparison Items		Legendre	Zernike	Tchebichef	Krawtchouk	Wavelet	Curvelet	GLCM	algorithm cost time(s)
Image (c)1	C_{ACC}	0.8615	0.8450	0.8323	0.8032	0.9144	0.9468	0.8952	usual times (99.8s)
	C_{TPR}	0.9264	0.9263	0.9085	0.9112	0.9365	0.9622	0.9221	
	C_{FAD}	0.0088	0.0076	0.0154	0.0192	0.0488	0.0032	0.0892	
	C_{FPR}	0.0752	0.0795	0.0762	0.1080	0.0221	0.0219	0.0269	our method times (8.2s)
	C_{SI}	0.8545	0.8489	0.8442	0.8224	0.8332	0.9675	0.7932	
	Max energy subbands 1,26,25,27,2								
Image (c)2	C_{ACC}	0.8912	0.8566	0.8822	0.7986	0.9134	0.9268	0.8867	usual times (97.4s)
	C_{TPR}	0.9452	0.9568	0.9523	0.9025	0.9457	0.9690	0.9110	
	C_{FAD}	0.0081	0.0570	0.0225	0.0064	0.0097	0.0049	0.0233	
	C_{FPR}	0.0540	0.1002	0.0701	0.1039	0.0323	0.0216	0.0243	our method times (7.8s)
	C_{SI}	0.8967	0.8697	0.8899	0.8175	0.9048	0.9307	0.8321	
	Max energy subbands 26,25,27,1,28								
Image (c)3	C_{ACC}	0.2435	0.0143	0.1438	0.2224	0.9007	0.9029	0.8623	usual times (93.1s)
	C_{TPR}	0.3243	0.3538	0.4263	0.5503	0.9207	0.9572	0.8923	
	C_{FAD}	0.5949	0.3068	0.2913	0.1217	0.0027	0.0030	0.0891	
	C_{FPR}	0.0808	0.3395	0.2825	0.3279	0.0200	0.0528	0.0300	our method times (7.3s)
	C_{SI}	0.3000	0.2641	0.3324	0.4144	0.8229	0.9249	0.7531	
	Max energy subbands 1,26,25,27,2								
Image (c)4	C_{ACC}	0.8426	0.7787	0.8233	0.7146	0.9042	0.8933	0.8675	usual times (96.2s)
	C_{TPR}	0.9007	0.9079	0.9083	0.8571	0.9355	0.9365	0.9227	
	C_{FAD}	0.0012	0.0771	0.0333	0.0036	0.0332	0.0218	0.0222	
	C_{FPR}	0.0781	0.1492	0.1050	0.1425	0.0313	0.0420	0.0551	our method times (8.1s)
	C_{SI}	0.8540	0.8074	0.8401	0.7502	0.9071	0.8969	0.8744	
	Max energy subbands 26,25,27,1,2								
Image (c)5	C_{ACC}	0.8402	0.7299	0.8398	0.7833	0.8954	0.9130	0.8707	usual times (92.9s)
	C_{TPR}	0.8909	0.8292	0.8858	0.8822	0.9072	0.9536	0.8995	
	C_{FAD}	0.0583	0.0714	0.0681	0.0189	0.0965	0.0084	0.0564	
	C_{FPR}	0.0507	0.0994	0.0460	0.0989	0.0041	0.0377	0.0364	our method times (6.5s)
	C_{SI}	0.8479	0.7543	0.8469	0.8028	0.8958	0.9182	0.8753	
	Max energy subbands 27,26,25,1,28								
Image (c)6	C_{ACC}	0.7716	0.6876	0.7171	0.6904	0.8303	0.8644	0.8988	Usual times (97.3s)
	C_{TPR}	0.7951	0.7867	0.7950	0.8882	0.9930	0.9877	0.9681	
	C_{FAD}	0.1813	0.1142	0.1271	0.0860	0.1558	0.1116	0.0374	
	C_{FPR}	0.0235	0.0991	0.0779	0.1978	0.1628	0.1227	0.0693	our method times (6.8s)
	C_{SI}	0.7768	0.7158	0.7375	0.7415	0.8540	0.8787	0.9054	
	Max energy subbands 26,25,27,1,2								
Image (c)7	C_{ACC}	0.4037	0.3628	0.3670	0.4389	0.3497	0.9214	0.8497	Usual times (95.4s)
	C_{TPR}	0.6726	0.6632	0.6834	0.6665	0.6716	0.9379	0.9113	
	C_{FAD}	0.0585	0.0364	0.0018	0.1060	0.0066	0.0430	0.0272	
	C_{FPR}	0.2689	0.3004	0.3164	0.2276	0.3219	0.0149	0.0616	our method times (7.1s)
	C_{SI}	0.5301	0.5100	0.5191	0.5429	0.5080	0.9222	0.8584	
	Max energy subbands 27,26,25,1,30								

4. Conclusion

The ultrasound image segmentation method based on semi-supervised in curvelet domain is presented in this article, in this paper our work mainly include: Firstly ultrasound images are decompose into different frequencies and orientations through curvelet transform, then Cauchy distribution is used to simulate the curvelet coefficients distribution and main distribution curvelet coefficients are extracted for curvelet inverse transform, after inverse transform, accroding to the texture analysis we extract major energy direction sub-bands for the following features calculation, these features mainly include: angular second moment, contrast, correlation, entropy. therefore, our algorithm time-consuming degree is reduced. Secondly eigenvectors composed by these features are taken into the SVM

© 2012 NSP
Natural Sciences Publishing Cor.

classifier to complete the image segmentation based on the semi-supervised learning thoughts. Finally experimental results show that our method can accurately extract the pathological region of the ultrasound images. In the future work, the authors intend to undertake further research in the time-Frequency analysis and study in machine learning domain, commit ourselves to put forward more accurate and more real-time ultrasound image segmentation method.

Acknowledgement

The authors acknowledge the financial support National Key Basic Research Program Project 973 , project No. (2011CB707904); High academic qualifications fund of Nanjing Forestry University , project No. (163070052, 163070036). The author is grateful to the anonymous referee for a careful checking of the details and for helpful comments that improved this paper.

References

[1] Z.Iscan, M.N.Kurnaz and Z.Dokur, Neural Infor Proc **10**, 183 (2006).
[2] S.Yan, J.P.Yuan and C.H.Hou, Proc. 2010 International Conference on Advanced Computer Theory and Engineering, 85 (2010).
[3] A.Kermani and A.Ayatollahi, Biomedical Sci and Eng **3**, 1078 (2010).
[4] J.Xie, Y.Jiang and H.T.Tsui, IEEE Trans Medical Imag **24**, 539 (2005).
[5] M.Hlne, R.Cardinal and J.Meunier, IEEE Trans Medical Imag **25**, 590 (2006).
[6] L.Grady and G.Funka-lea, LNCS **3117**, 230 (2004).
[7] D.Cremers, M.Rousson and R.Deriche, Compute Vision **72**, 195 (2007).
[8] I.Dydenko, F.Jamal, O.Bernard and J.D'hooge, Medical Imag Analysis **10**, 162 (2005).
[9] A.Sarti, C.Corsi, E.Mazzini and C.Lamberti, IEEE Trans Ultrasonics, Ferroelectronics and Frequency Control **52**, 947 (2005).
[10] C.I.Christodoulou, C.S.Pattichis, IEEE Trans Medical Imag **22**, 902 (2003).
[11] E.J.Cands, L.Demanet, D.L.Donoho and L.Ying, Multiscale Modeling Simulation **5**, 861 (2006).
[12] E.J.Cands and L.Demanet, Commun on Pure and Applied Mathematics **58**, 1472 (2005).
[13] K.Wu, C.Garnier and J.L.Coatrieux, Proc. 2010 IEEE Engineering in Medicine and Biology Society Conference, 5581 (2010).
[14] V.S.Vyas and P.P.Rege, ICGST-BIME Journal **7**, 29 (2007).
[15] N.Qaiser, M.Hussain and A.Hussain, International Journal of Computer Science and Network Security **8**, 264 (2008).
[16] L.Dettori and L.Semler, Comput in Biology and Medicine **37**, 486 (2007).

Ting Yun is a Lecturer of Nanjing Forestry University, and as the postdoctor to carry on research on medical image analysis in Southeast University, his main research direction include: Mathematics and image processing, Pattern recognition, Graphic analysis of three-dimensional modeling. he obtained his doctorate from Nanjing University of Science and Technology (CHINA) and published more than ten academic articles.

© 2012 NSP
Natural Sciences Publishing Cor.